The Role of Chain-Length Distribution in the Formation of Solid-State Structures of Polypeptide-Based Rod−Coil Block Copolymers

Helmut Schlaad,* Bernd Smarsly, and Magdalena Losik

Max Planck Institute of Colloids and Interfaces, Colloid Department, Am Mühlenberg 1, 14476 Golm, Germany

Received December 3, 2003; Revised Manuscript Received January 21, 2004

ABSTRACT: The structural details of thick polymer films made from poly(Z-L-lysine)−polystyrene rod−coil block copolymers, the polydispersity index being in the range ∼1.01−1.64, were investigated by small-angle X-ray scattering techniques. All films were found to have a hexagonal-in-zigzag lamellar morphology. The zigzag superstructure, a plane lamellar structure disrupted by kinks, results from the hexagonal packing of the polydisperse set of polypeptide α-helices, fractionated according to the length of helices. The data reveal a correlation between the molecular weight distribution of the polypeptide and the interface−curvature properties of the morphology.

Introduction

Synthetic polypeptide-based block copolymers usually exhibit the phase behavior of rod−coil block copolymers, which is due to the fact that α-helical polypeptides act as rodlike mesogens.[1−5] Virtually all materials examined show a very strong preference for lamellar structures in the solid state.[6−12] The only exceptions reported so far are symmetric triblock copolymers with a short central polybutadiene segment ("once-broken rods"), forming spherical or cylindrical domains in a matrix of hexagonally arranged polypeptide helices,[13−15] and peptide-based diblock oligomers, self-assembling into a "double-hexagonal" morphology.[16]

Gallot et al.[6−9] were the first to investigate the solid-state structures of polyvinyl−polypeptide diblock copolymers employing small-angle X-ray scattering (SAXS), transmission electron microscopy (TEM), infrared (IR), and circular dichroism (CD) spectroscopy. Regardless of the volume fractions of comonomers (0.15−0.75), polymers were found to self-assemble into a lamellar morphology of alternating polyvinyl and polypeptide sheets. The spacing between sheets (*d*) was 25−35 nm, weakly depending on the molecular weight of the copolymer. In addition to this lamellar superstructure, the α-helical polypeptide chains (18_5-helix, 3.6 monomer units per turn) were arranged in a hexagonal array with a characteristic lattice spacing of $d_H \sim 1.5$ nm. A schematic drawing of the hexagonal-in-lamellar morphology of polyvinyl−polypeptide block copolymers is shown in Chart 1.

It is obvious that the hexagonal packing of α-helices excludes a regular antiparallel orientation of the dipole moments.[5] Hence, local dipole fields might restrict the maximal helix length to a few nanometers and promote a folding of the polypeptide chains. In fact, the thickness of polypeptide layers, as determined by SAXS, was always smaller than the contour length of the α-helix. Depending on the molecular weight of the polypeptide, chains were interdigitated or folded up to seven times.

Gallot et al.[8,9] further reported three or more orders of sharp lamellar reflections in the X-ray diffraction

* Corresponding author: phone ++49.331.567.9514; Fax ++49.331.567.9502; e-mail schlaad@mpikg-golm.mpg.de.

Chart 1. Schematic Representation of the Hexagonal-in-Lamellar Solid-State Morphology of Polyvinyl−Polypeptide Block Copolymers
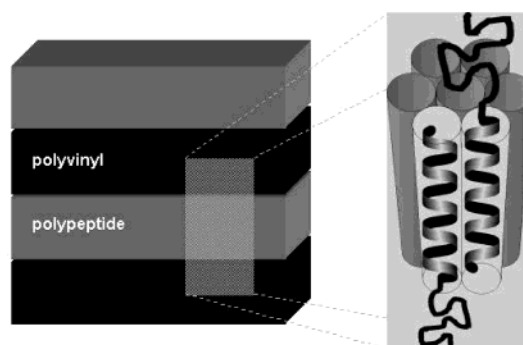
patterns, indicating a very high quality of lamellar order. This might be attributed to the fact that the stacks of polypeptide lamellae are very rigid and have an "infinite" persistence length. It is noteworthy that the copolymer samples used were carefully fractionated and thus had a nearly monodisperse molecular weight distribution (MWD). For films of nonfractionated samples, however, Schlaad et al.[12] obtained SAXS patterns which were rather ill-defined at very low angles often showing just a single broad peak (cf. Figure 1, top). Nevertheless, the long-range order in the films was very high, i.e., in the range of microns, as seen by TEM or atomic force microscopy (AFM) (see Figure 1, bottom). The apparent discrepancy between SAXS and TEM/AFM results could be explained with the existence of a hexagonal-in-undulated lamellar or zigzag morphology (see Chart 2). Here, stacks of lamellae are extended "infinitely", but the thickness of individual lamellae is statistically fluctuating. Such undulations are supposed to result from the hexagonal packing of a polydisperse set of polypeptide helices.

In the present work, we examined in more detail the role of the length distribution of helices in the formation of undulated lamellar structures of polystyrene−poly(Z-L-lysine) (PS−PZLLys) block copolymers. The solid films of five different copolymer samples varying substantially in polydispersity index (PDI = ∼1.01−1.64) were analyzed by means of SAXS. The concepts applied for the
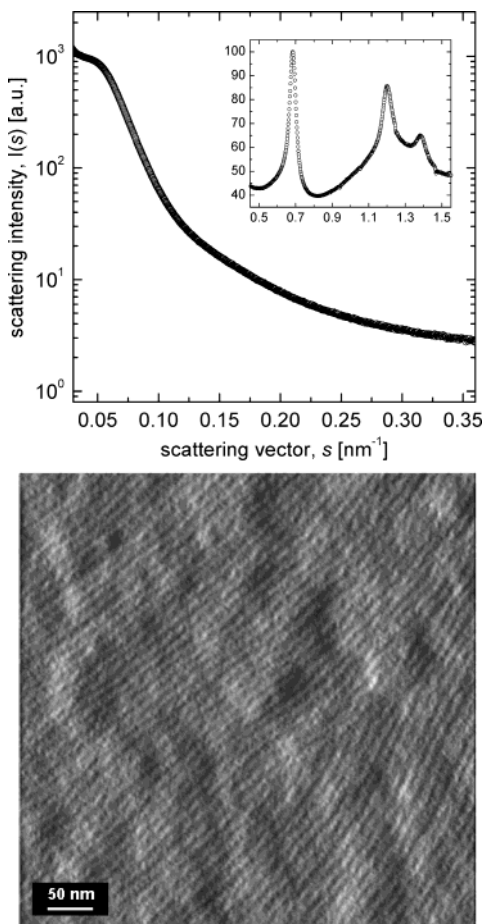
Figure 1. (top) Radial-averaged SAXS diffractogram of the DMF-cast film of PS−PZLLys sample **1** (Table 1); inset shows the pattern arising from the array of hexagonally packed PZLLys helices. (bottom) AFM amplitude image (0.5 × 0.5 μm, Z range: 25 mV) of the PS−PZLLys polymer film prepared by spin-coating a ~2 wt % solution of **1** in DMF on silicon. Note that lamellae are oriented perpendicular to the substrate.[10]

Chart 2. Schematic Representation of the Hexagonal-in-Undulated Lamellar Solid-State Morphology of Polydisperse Polyvinyl−Polypeptide Block Copolymers
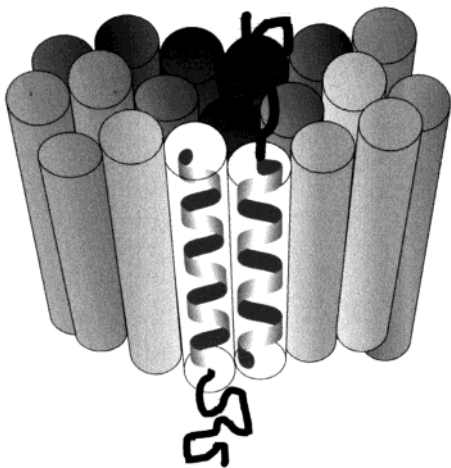
evaluation of the SAXS data were that of the *interface distribution function*[17] and the *κ−ι formalism*.[18] These two concepts make it possible to determine the thickness of individual layers and the interface−curvature properties of the lamellar structures, respectively.

Experimental Methods

The synthesis of PS−PZLLys block copolymers via ω-amino end-functional PS initiated ring-opening polymerization of ZLLys-*N*-carboxyanhydride in *N,N*-dimethylformamide (DMF) as the solvent has been described in detail elsewhere.[19,20] The chemical composition and number-average molecular weight (M_n) of copolymers were determined by ^{1}H NMR analysis (Bruker DPX-400 spectrometer operating at 400.1 MHz) in DMF-d_7 as the solvent at 25 °C. MWDs were accessed by size exclusion chromatography (SEC; eluent: *N,N*-dimethylformamide + 0.5 wt % LiBr at 70 °C; flow rate: 1 mL min^{-1}; stationary phase: 300 × 8 mm PSS-GRAM 10 μm columns (30, 30, 100, 3000 Å) (Polymer Standards Service GmbH, Mainz, Germany); detectors: TSP UV1000 (λ = 270 nm) and Shodex RI-71); the chromatograms were evaluated employing the SEC-UV/RI method described by Schlaad and Kilz.[21] Circular dichroism (CD) spectroscopy (JASCO J 715) was performed on ~0.03 wt % polymer solutions in tetrahydrofuran (THF) at 25 °C. The percentage of α-helix was estimated from the absolute values of the molar ellipticity, [Θ], at λ = 225 nm, based on the computed CD spectra for PLLys by Greenfield and Fasman.[22]

Polymer films were prepared by solvent casting from 5 to 10 wt % polymer solutions in DMF as a nonselective solvent. Liquid samples were placed on Teflon-coated aluminum foil (BYTAC) and were slowly dried within 12−24 h at 40 °C. The specimens were then scratched off the foil and isolated as powder. As described earlier,[12] changing the experimental protocol for solvent casting and/or subsequent annealing at 110 °C, i.e., above the glass transition temperature of PS, did not affect the morphology of the films.
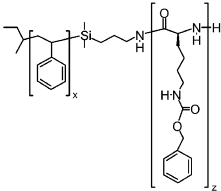
SAXS curves were recorded at room temperature with a Nonius rotating anode instrument (4 kW, Cu Kα) with pinhole collimation and an image-plate detector. The distance between sample and detector was 40−140 cm, covering a range of the scattering vector $s = 2/\lambda \sin \theta = 0.02−1.6$ nm^{-1} (2θ = scattering angle, λ = 0.154 18 nm). 2D diffraction patterns were transformed into a 1D radial average of the scattering intensity. Further details are given in ref 23.

Results and Discussion

For the synthesis of the PS−PZLLys block copolymer samples **1**−**5**, the identical ω-amino end-functional PS (average number of styrene units, x = 52; PDI = 1.03) was used to initiate the ring-opening polymerization of ZLLys-*N*-carboxyanhydride in DMF solution; experimental details are given elsewhere.[19,20] The mole fraction (f_z = 0.43−0.68) and number of ZLLys units (z = 40−111) of the copolymers were determined by ^{1}H NMR, and the absolute MWDs were accessed by SEC (PDI = ~1.01−1.64; cf. Figure 2).[21] The molecular characteristics of samples **1**−**5** are summarized in Table 1.

The radial-averaged SAXS curves obtained for the DMF-cast films of PS−PZLLys samples **1**−**5** are shown in Figure 3. Only a single peak could be observed at low values of the scattering vector, s < 0.2 nm^{-1}, regardless of the MWD of the copolymer sample. Considering a lamellar morphology of the films (cf. Introduction), the peak maximum is a measure of the long period or intersheet spacing (d)—the results for **1**−**5** are listed in Table 2. In addition, the SAXS diffractograms at s > 0.6 nm^{-1} (cf. Figure 1) usually showed three peaks with a characteristic Bragg spacing in the ratio 1:3$^{0.5}$:2, originating from the hexagonal packing of PZLLys α-helices (d_H ~ 1.5 nm, i.e., distance between helices is ~1.7 nm).[9,12] According to CD spectroscopy, the α-helix content of PZLLys should be in the order of 65% (**1**) and 80−95% (**2**−**5**). Note that **1** is the only

Table 1. Molecular Characteristics of PS−PZLLys Block Copolymers under Study

chemical structure	sample	x^a	z^b	$f_z{}^c$	PDI^d	% helix^e
	1	52	69	0.57	1.64	65
	2	52	111	0.68	1.27	90
	3	52	60	0.54	1.24	90
	4	52	50	0.49	~1.01	95
	5	52	40	0.43	~1.01	85

^{a} Number-average degree of polymerization of the PS block segment; size exclusion chromatography (SEC). ^{b} Number-average degree of polymerization of the PZLLys segment; ^{1}H NMR. ^{c} Mole fraction of ZLLys in the copolymer. ^{d} Polydispersity index; SEC−UV/RI.[21] ^{e} Estimated percentage of α-helix; circular dichroism spectroscopy (CD).[22]
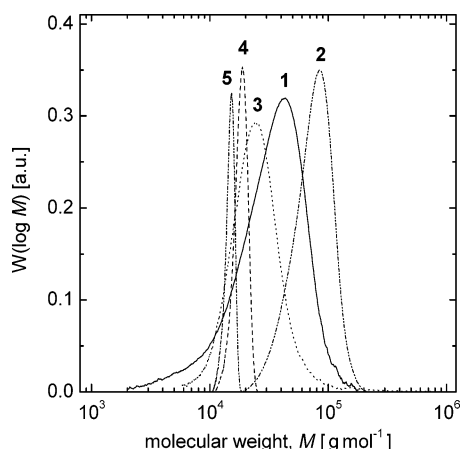
Figure 2. Mass distributions of the PS−PZLLys samples **1**−**5** (Table 1), as determined by size exclusion chromatography (SEC-UV/RI method).[21]
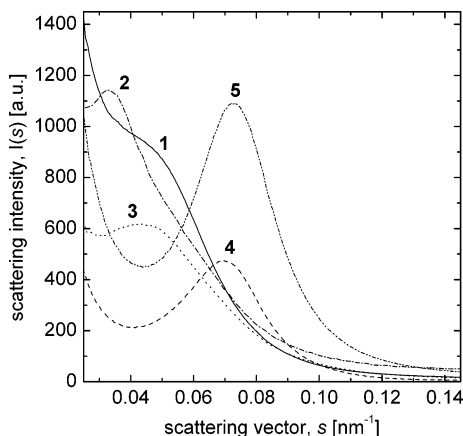
Figure 3. Radial-averaged SAXS curves of the polymer films cast from PS-PZLLys samples **1**−**5**.

sample containing considerable amounts of copolymer chains with less than 15 ZLLys units (∼5 mol %, estimated from the SEC frequency distribution), which are not able to form stable α-helices.[24]

To depict further details of the nanometer-scale morphology of these films, the SAXS data were analyzed to determine the thickness of the PS and PZLLys layers, d_S and d_L, respectively ($d = d_S + d_L$). These parameters can be obtained from SAXS data via the concept of interface distribution function introduced by Ruland.[17] The approach provides the so-called Porod's length, l_p,

Table 2. Results of SAXS Analysis of PS−PZLLys Block Copolymer Films 1−5

sample	$\phi_L{}^a$	d (nm)^b	d_S (nm)^c	d_L (nm)^c	κ^d	ι^d
1	0.74	16.7	4.5	12.2	1.2 ± 0.1	2.0 ± 0.2
2	0.82	29.4	4.8	21.7	1.9 ± 0.2	2.2 ± 0.2
3	0.71	14.1	3.5	10.6	1.8 ± 0.2	2.0 ± 0.1
4	0.68	13.4	3.7	9.7	1.0 ± 0.1	2.0 ± 0.1
5	0.63	12.1	3.9	8.2	0.8 ± 0.1	2.0 ± 0.1

^{a} Volume fraction of ZLLys in the copolymer.[12] ^{b} Long period or intersheet spacing. ^{c} Thickness of individual layers: PS (d_S) and PZZLys (d_L), experimental error: ±10%.[17] ^{d} Normalized scattering-average of curvature (κ) and averaged normalized interface area (ι).[18]
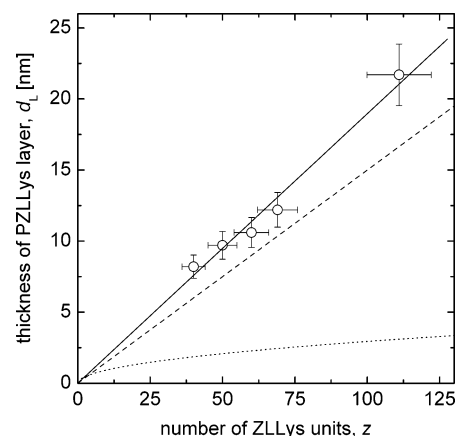
Figure 4. Dependence of the number-average thickness of PZLLys layers (d_L, SAXS) on the number-average number of ZLLys units (z, NMR) in the copolymer. Solid line: linear fit through experimental data; slope: 0.19 ± 0.01 nm. Dashed line: $d_L/\text{nm} = 0.15z$, calculated line assuming a fully extended α-helix with a projected length of a ZLLys segment of 1.5 Å.[9] Dotted line: $d_L/\text{nm} \sim 2R_g = (2/3)^{0.5} l_L z^{0.5}$, calculated line assuming random coil conformation of PZLLys (R_g: radius of gyration; l_L: length of a ZLLys segment = 3.6 Å).

which is correlated with the thickness of the layers by

$$d_S = l_p/2\phi_L \tag{1a}$$

$$d_L = l_p/2(1 - \phi_L) \tag{1b}$$

(ϕ_L = volume fraction of the PZLLys block; see Table 2). The results obtained for the films **1**−**5**, applying the approach described by Smarsly et al.,[23] are summarized in Table 2. As can be seen in Figure 4, the thickness of the PZLLys layer, d_L, is linearly proportional to the number-average degree of polymerization[17] of the PZLLys block, z. The slope of the line graph indicates that the contribution of every ZLLys unit to the length of the helix is 1.9 Å, which is somewhat higher than the 1.5 Å calculated for a 100% crystalline polypeptide 18_5-helix.[9] The "streching" of the helix might be attributed to the presence of amorphous, partially unwinded or β strand regions (see above; contour length of an all-trans ZLLys unit: ∼3.6 Å). Note that the thickness of the layer should be considerably smaller and should scale with $z^{0.5}$ if the PZLLys segments were in a random coil conformation (see the dotted line in Figure 4). Here, the PZLLys lamellae are composed of a monolayer of interdigitated α-helices,[9] as illustrated in Chart 2, and the main axis of the helices is oriented perpendicularly to the PS−PZLLys interface. Backfolding of the helices, as described by Gallot et al.[9] for high-molecular-weight samples, can be excluded for samples **1**−**5**. Interdigitation and backfolding are ways to compensate the large
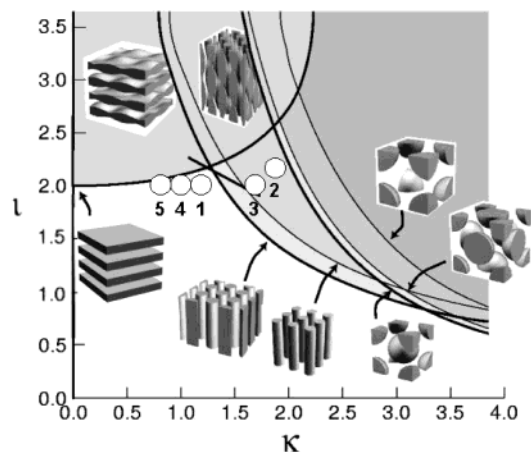
Figure 5. Experimental $\kappa-\iota$ data obtained for the PS−PZLLys films **1**−**5**, inserted in the generalized phase diagram.

dipole moments of α-helices ($\mu = 3.5$ D per unit)[25] and to minimize the energy of the PZLLys layers. However, as mentioned earlier, an effective mismatch of local dipole moments must be considered when helices are packed in a hexagonal array (in contrast to the situation in a tetragonal arrangement). It might therefore be expected that the thickness of PZLLys layers cannot exceed a certain limit. As can be seen from Figure 4, this limit should be well above ~20 nm.

SAXS data were further analyzed in terms of the $\kappa-\iota$ formalism described by Burger et al.,[18] which is designed for the treatment of two-phase systems with sufficiently strong segregation. The approach is based on the extraction of characteristic geometric quantities from experimental SAXS curves, in particular dimensionless parameters describing the interface curvature, κ, and the specific interface, ι, given by

$$\kappa = L\langle H^2 \rangle_S \qquad (2)$$

$$\iota = L(S/V) \qquad (3)$$

$L = 1/s^*$ is the period determined by the position of the first intensity maximum at $s = s^*$, $\langle H^2 \rangle_S$ is the squared mean curvature, and S/V is the interface area per unit volume. Note that the local interface and curvature properties are assumed to equilibrate rapidly and should not depend on the pathway of film processing.[12] These parameters can be quantified by a thorough analysis of the asymptotic Porod regime of the SAXS data and allow determination of the structure on the basis of a general phase diagram comprising the most prominent block copolymer mesophases (cf. Figure 5). Most importantly, this method is applicable even when SAXS curves show only a single broad reflection—like for the PS−PZLLys films **1**−**5**.

The results obtained from the $\kappa-\iota$ analysis of SAXS data are summarized in Table 2, and the experimental $\kappa-\iota$ values for **1**−**5** are inserted in the generalized phase diagram[18] shown in Figure 5. The value of the reduced specific interface was found to be $\iota = 2.0$ (**2**: $\iota = 2.2$), which is the expected value for a plane lamellar phase. Despite that, all structures exhibit a noticeable curvature, as indicated by the values of the reduced mean curvature, $\kappa = 0.8-1.9$. It is interesting to see that, taking into account the $\kappa-\iota$ phase diagram shown in Figure 5, lamellar structures with $\iota = 2.0$ and $\kappa > 1$ can exist at all. The most reasonable model of a structure
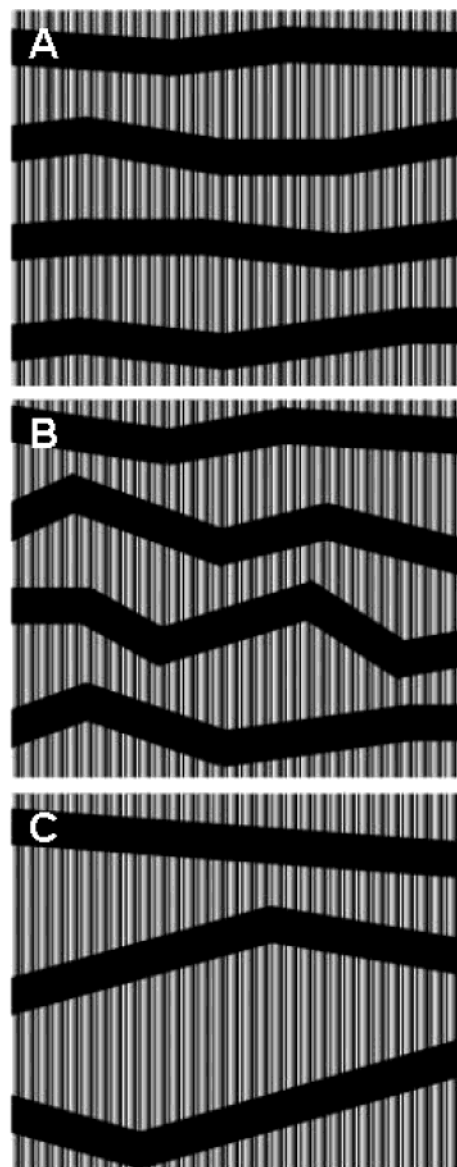

Figure 6. Schematic representation of the disordered zigzag lamellar morphology formed by polypeptide-based diblock copolymers with low (A), moderate (B), and high polydispersity (C) with respect to the length of helices. Polypeptide helices are represented as cylinders, and polyvinyl sheets are depicted in black.

exhibiting the given properties should be a disordered zigzag lamellar morphology as depicted in Figure 6. Note that a similar morphology on the 100−200 nm length scale has earlier been observed for a poly(hexyl isocyanate)−polystyrene rod−coil block copolymer system.[26] However, the generation of a plane PS−PZLLys interface ($\iota = 2.0$) between the "kinks" requires a fractionation of the copolymer chains according to length during casting of the film. Otherwise, a rough surface with a substantially larger interface area would have been formed, which for energy reasons is not favorable.

It is evident that the structures with the smallest value of the curvature parameter κ were produced by the copolymers **4** (1.0) and **5** (0.8), which exhibit a nearly monodisperse Poisson MWD (PDI < 1.03). Also, the width of the SAXS peaks is least for these samples. The highest values ($\kappa = 1.8-1.9$), on the other hand, were observed for the samples **2** and **3** with moderate PDI ~ 1.25. In fact, it is well expected that increasing the

variance in the length of the helices should produce larger fluctuations in the thickness of the PZLLys layers and more kinks, the latter contributing to the curvature of lamellae. The phase behavior of these samples can thus be rationalized as illustrated in Figure 6A,B. However, this seems to hold true as long as the entropic contributions to the free energy are greater than the interfacial tension between the PS and PZLLys layers. Note that the generation of a fluctuating thickness of layers is at the expense of a larger interface area. When the MWD of the copolymer sample is too broad, as in the case of sample **1** (PDI = 1.64), plane lamellae with an intermediate $\kappa = 1.2$ are formed. It is supposed that the dropping of the κ value is due to a decrease of the number of kinks per volume unit or, in other words, extension of the plane interfacial domains between two kinks (see Figure 6C). Fractionation of the copolymer chains occurs parallel to the interface; i.e., all PZLLys layers have the same average thickness. Thus, the existence of a plane lamellar structure consisting of uniform PZLLys layers, the thickness of which varying from layer to layer, can be excluded here. For such a structure, it should be $\iota = 2$ and $\kappa = 0$.

It is interesting to see that even for copolymers with a Poisson MWD, SAXS patterns are ill-defined and do not show higher orders of lamellar reflections. On the basis of the structure model described here, however, the situation should change when the PZLLys blocks are strictly monodisperse and can form a phase with a perfectly smectic order. We are currently working on the solid-phase synthesis of such PS−PZLLys block copolymers to verify this hypothesis. Having monodisperse samples at hand would also offer the possibility to learn more about the basic principles and energetics in the self-assembly processes of rod−coil block copolymers.

However, it has so far not been paid much attention to polydispersity when dealing with structure formation of rod−coil block copolymers. In fact, many of the systems being investigated were prepared by polycondensation reactions,[3] which usually produce polymers with a Schulz−Flory distribution (PDI = 2) or even broader MWD. Polydispersity effects might play a considerable role in these systems and explain deviations from the predicted phase behavior (cf. ref 27) or the appearance of unusual morphologies.

Summary

The PS−PZLLys coil−rod block copolymers under study ($f_z = 0.43−0.68$, PDI = ~1.01−1.64) were found to self-assemble into a hexagonal-in-zigzag lamellar solid-state morphology, as revealed by standard and curvature−interface ($\kappa−\iota$) analysis of SAXS data of DMF-cast thick films. Within the polypeptide layers, PZLLys α-helices are interdigitated and arranged in a hexagonal array. The average thickness of PZLLys layers is linearly proportional to the number of ZLLys units, the contribution per monomer segment being 1.9 Å. As a matter of the chain length distribution of the helices, the average thickness of PZLLys layers is not constant but statistically fluctuating. A fractionation of the helices according to length promotes the generation of an almost plane lamellar interface ($\rightarrow \iota = 2.0$), which is disrupted by kinks ($\rightarrow \kappa = 0.8−1.9$). The broader the length distribution of helices, the larger are the fluctuations in the PZLLys layer thickness, provided that the entropic contributions to the free energy are greater than the interfacial tension between PS and PZLLys layers. Evidently, this seems to hold true for samples with low or moderate polydispersity (PDI < 1.3). If the distribution is considerably broader (PDI = 1.64), minimizing of the interfacial area is accompanied by a decrease of the number of kinks.

References and Notes

(1) Chen, J. T.; Thomas, E. L.; Ober, C. K.; Mao, G.-P. *Science* **1996**, *273*, 343.
(2) Gallot, B. *Prog. Polym. Sci.* **1996**, *21*, 1035.
(3) Lee, M.; Cho, B.-K.; Zin, W.-C. *Chem. Rev.* **2001**, *101*, 3869.
(4) Klok, H.-A.; Lecommandoux, S. *Adv. Mater.* **2001**, *13*, 1217.
(5) Schlaad, H.; Antonietti, M. *Eur. Phys. J. E* **2003**, *10*, 17.
(6) Billot, J.-P.; Douy, A.; Gallot, B. *Makromol. Chem.* **1976**, *177*, 1889.
(7) Perly, B.; Douy, A.; Gallot, B. *Makromol. Chem.* **1976**, *177*, 2569.
(8) Billot, J.-P.; Douy, A.; Gallot, B. *Makromol. Chem.* **1977**, *178*, 1641.
(9) Douy, A.; Gallot, B. *Polymer* **1982**, *23*, 1039.
(10) Gervais, M.; Douy, A.; Gallot, B.; Erre, R. *Polymer* **1988**, *29*, 1779.
(11) Janssen, K.; van Beylen, M.; Samyn, C.; Scherrenberg, R.; Reynaers, H. *Makromol. Chem.* **1990**, *191*, 2777.
(12) Schlaad, H.; Kukula, H.; Smarsly, B.; Antonietti, M.; Pakula, T. *Polymer* **2002**, *43*, 5321.
(13) Nakajima, A.; Hayashi, T.; Kugo, K.; Shinoda, K. *Macromolecules* **1979**, *12*, 840.
(14) Kugo, K.; Hayashi, T.; Nakajima, A. *Polym. J.* **1982**, *14*, 391.
(15) Hayashi, T.; Chen, G. W.; Nakajima, A. *Polym. J.* **1984**, *16*, 739.
(16) Klok, H.-A.; Langenwalter, J. F.; Lecommandoux, S. *Macromolecules* **2000**, *33*, 7819.
(17) Ruland, W. *Colloid Polym. Sci.* **1977**, *255*, 417.
(18) Micha, M. A.; Burger, C.; Antonietti, M. *Macromolecules* **1998**, *31*, 5930.
(19) Dimitrov, I.; Schlaad, H. *Chem. Commun.* **2003**, 2944.
(20) Dimitrov, I.; Kukula, H.; Cölfen, H.; Schlaad, H. *Macromol. Symp.*, in press.
(21) Schlaad, H.; Kilz, P. *Anal. Chem.* **2003**, *75*, 1548.
(22) Greenfield, N.; Fasman, G. D. *Biochemistry* **1969**, *8*, 4108.
(23) Smarsly, B.; Antonietti, M.; Wolff, T. *J. Chem. Phys.* **2002**, *116*, 2618.
(24) Kricheldorf, H. R. *Alpha-Aminoacid-N-Carboxyanhydrides and Related Heterocycles*; Springer: Berlin, 1987.
(25) Hol, W. G. J.; Vanduijnen, P. T.; Berendsen, H. J. C. *Nature (London)* **1978**, *273*, 443.
(26) Chen, J. T.; Thomas, E. L.; Ober, C. K.; Hwang, S. S. *Macromolecules* **1995**, *28*, 1688.
(27) Li, W.; Gersappe, D. *Macromolecules* **2001**, *34*, 6783.

MA035819M